The Dynamic Simulation of Automobile Accessory Drives

Dr.-Ing. Peter Solfrank and Dipl.-Ing. Peter Kelm

The Dynamic Simulation of Automobile Accessory Drives

Dr.-Ing. Peter Solfrank and Dipl.-Ing. Peter Kelm

The number of performance enhancing features in modern automobile accessory drives has increased over the past few years just as much as the cyclic irregularity of the crankshaft (due to the popularity of diesel motors and dual-mass flywheels). Nonetheless, the requirements for quiet operation and comfort are constantly on the rise. In spite of simple modeling and the use of well-known algorithms, the procedure discussed in this paper represents an efficient aid in predicting the dynamic behavior of accessory drives.
It allows a significant reduction in the experimental effort required in developing these systems. Simple operation and the clear representation of results, including animation, as well as quick calculations are the decisive criteria for the designer when using this tool.

1 Introduction

The days when a simple V-belt was used to drive the alternator from the crankshaft are long gone. Today, poly-V belts provide drive power for more than just the alternator and the water pump. They are also used to drive the steering pump, an air conditioner compressor and maybe a fan or even the oil pump. Considering the distribution of these drive units in the combustion engine and the length of the belt required, this is not possible in most cases without some kind of tensioning system. In addition, the increasing electrification of the automobile has lead to ever increasing alternator masses. The popularity of diesel engines and dual-mass flywheels has resulted in a sharp increase in the cyclic irregularity of the crankshaft as the driving vibration excitation for the belt. Finally, customer requirements for quiet operation and comfort are increasing sharply, while at the same time, a great deal of effort is made to suppress other sources of noise in the engine. Besides traditional design procedures – which, by the way, now also include higher requirements – such as belt life – dynamic problems must thus be considered as early as the design stage. Dynamic issues may even become a decisive quality criterion in the course of developing an application.

If the appropriate hardware is not yet available, calculated simulation is often required to draw reasonable conclusions about the dynamics of the adherent accessory belt drive. Previously, affordable means of simulation were not available to the design engineer in a suitable form, i.e. as an aid in the design process. The procedure discussed in this paper is based on simple and well-known model elements and mathematical algorithms. Many of the subsystems used have been discussed in detail in the literature (e.g. [1], [2], [3]). Although the discussion in [2] regarding the problem of slip between the belt and the pulley is much more thorough than in this paper, the proposals made there are not sufficient for the application treated here since many of the requirements are not met, in particular the dominance of nominal loads on the belt span as compared to vibration amplitudes. For the procedure to be discussed below, other model elements such as hydraulic tensioning elements are derived from a phenomenological standpoint without sacrificing meaningful conclusions. The numerical treatment of the procedure is sometimes even simplified by this approach.

Considering the simple modeling involved and the few adjustments made to the problem of numerical algorithms, the minimization of operational steps is characteristic for the approach described here. This means that this development tool is also user-friendly for the occasional user. Arbitrary combinations of model elements allow the designer a great deal of variation in his development work. The developed software also includes a three-dimensional animation of calculation results. This ensures that results can be viewed clearly and allows dynamic phenomena in the interaction of various subsystems to be studied in detail.

The components of the procedure discussed in this paper are first described, and calculation results are then compared with test results to verify the practical use of this approach.

2 Mechanical Model

2.1 General

In this paper, it is assumed that the belt drive is a planar system. The most important elements of the model include the following:

- belt pulleys with fixed axis and specified rotation
- belt pulleys with fixed axis and one rotational degree of freedom as well as a time-dependent or angle-dependent load torque
- belt spans as idealized spring/damper elements (Kelvin-Voigt model)
- belt spans capable of transversal vibrations
- belt pulleys whose axis of rotation is on a lever, which in turn rotates around a fixed point
- "mechanical" tensioning systems: This kind of system consists of a lever (with its own rotational degree of freedom). A tension pulley is positioned on the lever. In addition to the torque acting on the lever that results from belt forces through the tension pulley, the lever is also subjected to frictional torque and a torque resulting from the tensioning spring.
- "hydraulic" tensioning systems: In this case, the lever the tension pulley is on is affected by a translational spring element. The element's spring force, its damping and the nonlinear kinematics must all be considered. Damping, however, affects lever rotation in one direction only (due to a check valve).

Other elements representing rotational connections between pulleys make the model 3-dimensional in a nominal sense, although this does not detract from the simplicity of the planar model:

- rotating springs with viscous and/or Coulomb friction
- one-way clutch elements

A simplification is possible as long as the discussion is restricted to stationary operating conditions, i.e. constant average speeds of the drive pulley. Calculation can then be reduced to the deviations from that nominal motion.

2.2 Pulleys with and without rotational degrees of freedom

In practical applications, pulley rotation is most often specified using time series or Fourier series. This is typically the case for the crankshaft since it represents the vibration excitation and the system boundary simultaneously. The assumption is made that a reciprocal effect of the belt drive system on this boundary condition, i.e. on the rotation of the crankshaft, is negligible.

It is particularly advantageous to use a time series when measured values are available for the engine under investigation whose entire frequency contents are to be used. Here, a reference configuration is normally assumed, and several belt drive variants or tensioning system designs are analyzed. In other applications, the aim is to evaluate a concept without the aid of previous data, which often results in taking recourse to data based on "similar" engines. If this is the case, the best way to specify the cyclic irregularity of the crankshaft is to use a Fourier series that is reduced to a few harmonic components.

The mathematical representation of pulleys having a rotational degree of freedom poses no problems either since the simplest form of the angular momentum equation for these subsystems is valid for known torques. In addition to the

torques transmitted from the belt to the pulley (see below), there are also load torques for accessory drive belt pulleys. These torques are almost exclusively regarded as being constant with respect to time; even though this is not always the case, only insufficient information is available on their exact time behavior. Nonetheless, load torques can also be specified with respect to time or position in the computer program developed.
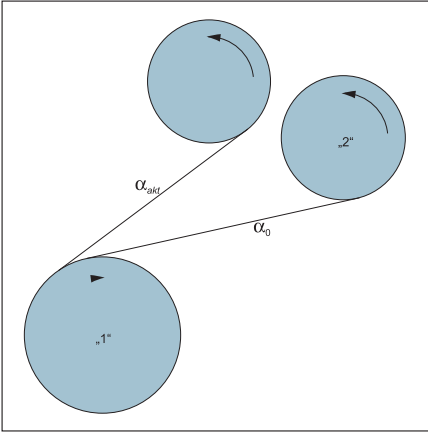
Figure 1   Belt span geometry

2.3 Belts without transversal vibrations

Regardless whether slippage between belt and pulley is provided for on the pulleys joined by a belt span, the representation of belt forces for the linearly elastic elongation behavior of the belt is comparatively trivial if no transversal vibrations are allowed in modeling.

For positions $\vec{x}_1$ and $\vec{x}_2$ of the pulley centers, the resulting angle a between the connecting line $\vec{x}_M$ and the direction $\vec{e}_{Rie}$ of the belt becomes

$$\alpha = \arcsin\left(\frac{d_1\, r_1 - d_2\, r_2}{|\vec{x}_M|}\right) \qquad (1)$$

where the free belt length l is

$$l = |\vec{x}_M|\, \cos\alpha \qquad (2)$$

The factor d_i (± 1) accounts for the nominal rotating direction of the pulley and r_i represents the radius of the pulley (Figure 1).

Comparing these quantities for the nominal and current condition yields the following calculation for belt elongation:

$$\Delta l = l_{akt} - l_0 + d_1 r_1 (\alpha_{akt} - \alpha_0 - \varphi_1) - d_2\, r_2\, (\alpha_{akt} - \alpha_0 - \varphi_2) \qquad (3)$$

Using the speeds of the belt and pulley contact points

$$\vec{v}_{k,\,i} = \vec{v}_{M,\,i} + d_i\, r_i\, \omega_i\, \vec{e}_{Rie} \qquad (4)$$

calculation for the elongation speed becomes

$$\frac{d}{dt}\Delta l = |\vec{v}_{k,\,2} - \vec{v}_{k,1}| \qquad (5)$$

Based on a Kelvin-Voigt model for the belt with the length-specific stiffness values and damping values EA and DA respectively, the current belt force is obtained

$$F = \max\left(0,\, F_0 + \frac{EA}{l_0}\,\Delta l + \frac{DA}{l_0}\,\frac{d}{dt}\,\Delta l\right) \qquad (6)$$

2.4 Belts with transversal vibrations

Modeling the transversal vibrations of the belt as string vibrations of the free spans is very similar to the representation given in [1]. Longitudinal vibrations are disregarded here. Although the longitudinal force of the belt in the free span is time dependent, it is regarded constant in the longitudinal direction. Omitting the damping terms yields a partial differential equation that can be used to describe the forces acting on an infinitesimal belt element:

$$\rho A\,\frac{\partial^2 y}{\partial t^2} + 2\,\rho A v\,\frac{\partial^2 y}{\partial x \partial t} - (F - \rho A v^2)\,\frac{\partial^2 y}{\partial x^2} + EI\,\frac{\partial^4 y}{\partial x^4} = 0 \qquad (7)$$

The symbols used in the formula signify the following:

ρA length-specific mass

y   amplitude of the belt element perpendicular to the tangent on the belt pulleys

x   longitudinal coordinate of the belt element

v   belt speed in the longitudinal direction

F   belt longitudinal force
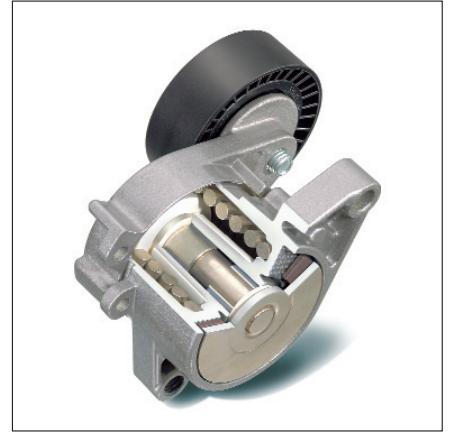
EI belt bending stiffness

Figure 2   Mechanical belt tensioning system

Using shape functions for the transversal motion of the belt based on the method proposed by Ritz

$$y(x, t) = w^T(x)\, q(t) \qquad (8)$$

with a vector w of purely spacial shape functions and the vector q or purely time-dependant functions, which represent degrees of freedom in the overall model, yields a representation transformed into ordinary differential equations:

$$M\ddot{q} + (G + D)\dot{q} + Kq = 0 \qquad (9)$$

with

$$M = \mu \int w\, w^T dx \qquad (9a)$$

$$G = 2\,\mu v \int w\, w'^T dx \qquad (9b)$$

$$D = \delta \int w'\, w'^T dx \qquad (9c)$$

$$K = (F - \mu v^2) \int w'\, w'^T dx \\ + EI \int w''\, w''^T dx \qquad (9d)$$

$$F = F_0 + \frac{EA}{l} \left(\frac{1}{2} q^T \int w'\, w'^T dx\ q + \Delta l \right) \\ + \frac{DA}{l} \left(q^T \int w'\, w'^T dx\ \dot{q} + \frac{d}{dt}\, \Delta l \right) \qquad (9e)$$

Damping proportional to velocity was added here, and its matrix formulation was based on the stiffness matrix. Pulley axes are assumed to be stationary. In calculating the longitudinal force of the belt according to formula (9e), the similarity to the calculation discussed in the last section (formula (6)) becomes apparent: The only difference is that changes in length and corresponding elongation speeds have been added due to the transversal vibrations.

Sine functions are used as shape functions for the transversal with their wavelength adjusted in such a way that a whole number multiple of half of the wavelength corresponds to the free length of the belt span:

$$w_i(x) = \sin\left(i\, \frac{\pi}{l_0}\, x\right)$$

This allows the local integral matrices to be given. For the j th shape function, the following ordinary differential equation results:

$$\frac{\mu\, l_0}{2} \ddot{q}_j + 4\,\mu v j \sum_{k\,=\,mod_2\,(j)\,+1}^{n,\ step\ 2} \frac{k\,\dot{q}_k}{j^2 - k^2} + \delta\, \frac{(j\pi)^2}{2l_0}\,\dot{q}_j \\ + \left[(F - \mu v^2)\, \frac{(j\pi)^2}{2l_0} + EI\, \frac{(j\pi)^4}{2l_0^3} \right] q_j = 0 \qquad (10)$$

2.5 Mechanical Tensioners

As was mentioned above, a system designated as a "mechanical" belt tensioner from an application engineering standpoint represents a lever that is driven by a torsion spring and damped by a Coloumb frictional torque (Figure 2). The torsion spring that applies the tensioning torque also introduces longitudinal force in the direction of the tensioner axis. This force acts on a ring surface equipped with a friction lining. This allows a nearly constant frictional torque about the axis of rotation.

For the representation of the overall system, this means that the number of degrees of freedom in the system can change depending on whether or not the frictional torque is sufficient to lock the lever. In the locked condition, the actual frictional torque compared to the maximum value achievable is reduced enough so that it compensates the other torques present. Determining current condition in the tensioning system (lever degree of freedom active or locked) as well as the current frictional torque in the locked condition is comparatively trivial in such a clear system as the one under investigation here.
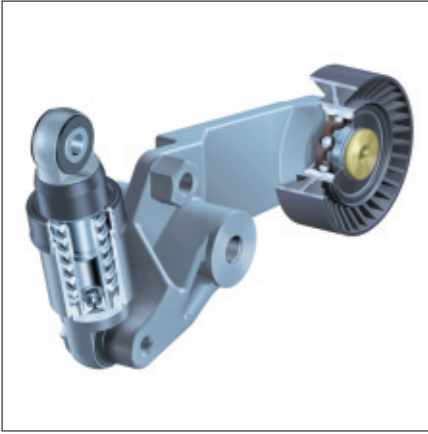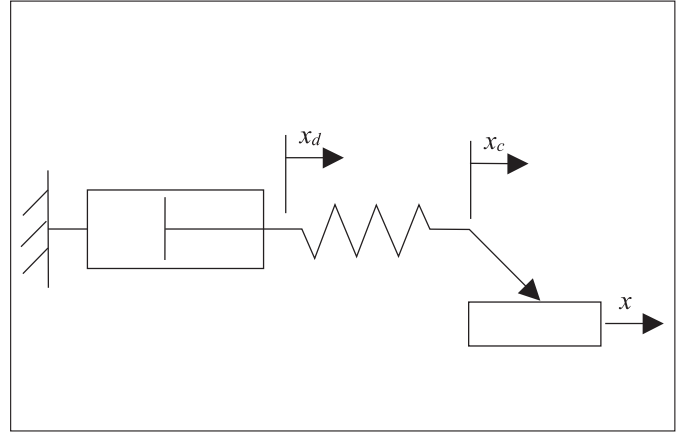
Figure 3   Hydraulic tensioning system

Figure 4   Mechanical model of the hydraulic tensioning element

2.6 Hydraulic Tensioners

The "hydraulic" tensioner already described (Figure 3) consists of a double lever with a rotating degree of freedom and a tensioning element installed between a point on the lever and an inertial point. The tensioning element collects forces in its longitudinal direction. There is a tensioning force caused by a preloaded spring, and there is a damping force that – due to a check valve – acts only in the direction of the contraction of the tensioning element.

In contrast to the theoretically resulting force displacement diagram for the sine-shaped excitation of a unilateral damper, measurements deviate from the purely speed-dependent damping effect. The mapping approximated in this representation is a slanted semi ellipse that results from the compressibility of the fluid in the damper and/or the elasticity of the damper housing or other flexible elements in the force flow.

The easiest way to represent this kind of behavior is to use a series connection of the ideal damper with a spring stiffness and a one-way clutch. The check valve serves to transmit forces in one direction only (Figure 4).

The force applied by this model element is:

$$F = c\,(x_d - x_c) = d\dot{x}_d \tag{11}$$

and the change in force with respect to time can be expressed as:

$$\dot{F} = c\,(\dot{x}_d - \dot{x}_c) = c\left(\frac{F}{d} - \dot{x}_c\right) \tag{12}$$

To represent this behavior in the scope of the system of differential equations to be solved, one internal degree of freedom for the force element is required in addition to the position and velocity of the conjoined points. In contrast to the system's other degrees of freedom, which correspond to second order differential equations in the mathematical model, only a single quantity is sufficient here since the description involves a first-order differential equation. This can be either a displacement or the force itself.
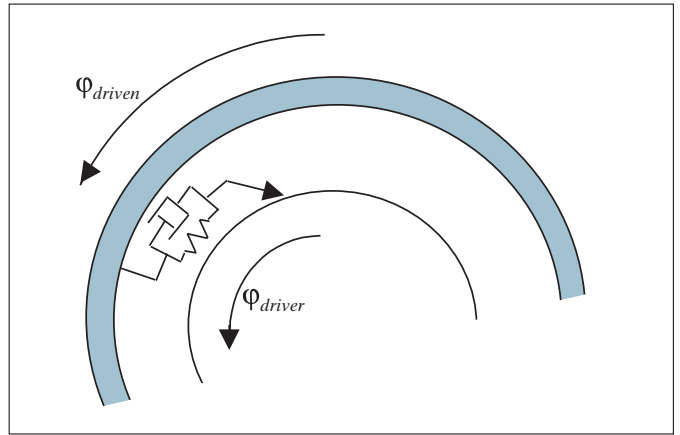
Figure 5   Model of the one-way clutch

2.7 Slippage between Belt and Pulley

For belt forces acting fully on the pulleys in the rotational direction, a sufficient grip between belt and pulley would be required. In reality, however, this is not the case. Instead, force transmission takes place on a more or less large portion of the belt wrap. Some of these processes are discussed at length in the literature, but a great deal of research into highly dynamic operating conditions remains incomplete (e.g. [2]). In spite of this, the resulting models are complex enough to make them unsuitable for a simple dynamic simulation.

A greatly simplified model is used for the task discussed in this paper by adjusting the classic rope friction equation according to Eytelwein. For the two belt forces bordering the belt wrap angle β, the following auxiliary condition applies:

$$F_{max} \leq (F_{min} - \rho Av^2)\, e^{\mu\beta} - \rho Av^2 \qquad (13)$$

where μ, is the coefficient of friction, ρA the length-specific belt mass and v the circumferential velocity of the belt. The auxiliary condition can be implemented in such a way that an additional degree of freedom is introduced for every pulley on which slip is to be possible. This degree of freedom represents the displacement of belt and pulley with respect to each other. If the auxiliary conditions are violated, there is an iterative adjustment of the additional degrees of freedom until a permissible condition is reached for the system. This corresponds to the slipping of the belt on the pulley.

2.8 The One-way Clutch

As already mentioned in the introduction, the cyclic irregularity of the crankshaft represents the root excitation of the accessory belt drive. The belt has the tendency to transmit both crankshaft acceleration and deceleration to the accessories. These alternate at a very high frequency. The high rotating inertia of the alternator in particular (increased by the high transmission to this accessory drive) leads to excessive belt forces and to a greater tendency to slip in the deceleration phase of cyclic irregularity. The result is an increased potential for the part to wear.

Thus, more and more alternator pulleys are being equipped with one-way clutches so that the sluggish alternator armature can be disengaged during the deceleration phase. This has two advantages. One the one hand, the corresponding torque transmission is eliminated in the deceleration phase, and on the other hand, the alternator's acceleration requirement in the next oscillation cycle is reduced since the deceleration of the crankshaft has not been. Instead, the alternator has only been subjected to its load torque. This effect is apparently most obvious whenever large cyclic irregularities in the excitation are accompanied by low alternator loads.

The mechanical model of the alternator overrunning device consists of a speed-dependent damping and a parallel arranged, nonlinear stiffness for torque transmission, which intervenes only when the speed of the driven pulley is lower than that of the driving pulley (Figure 5).

For the nonlinear stiffness, measurements suggest there is a relation between torque and deflection that can be expressed as $M = c_{Fl}\,\varphi_{Fl}^{el}$. However, the parameters for this must be determined experimentally for every clutch design.

In addition to this part of the clutch model, a speed-dependent damping that is constantly engaged is positioned in order to represent the clutch's drag torque in the overrunning mode. A formulation for the torque that is proportional to the relative speed usually yields satisfactory results. In some cases though, a Coloumb term was also used.
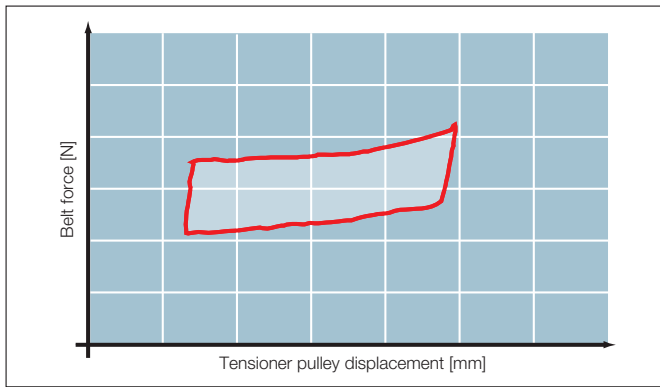
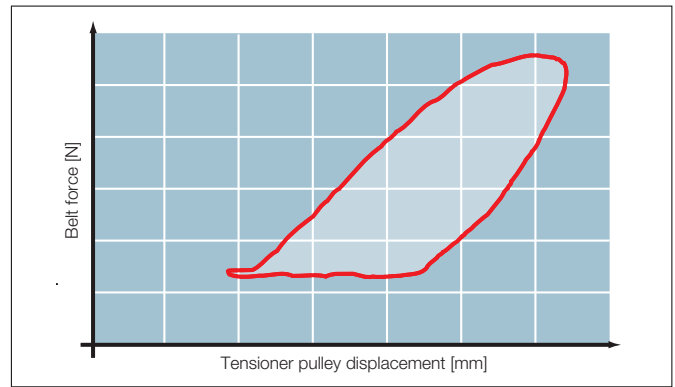Figure 6a   Mappings for mechanical tensioning systems

Figure 6b   Mappings for hydraulic tensioning systems

3 Implementation

Traditional integration procedures with adaptive stepsize control are used to integrate the equations of motion. In addition to various Runge-Kutta methods, comprehensive comparative computations have shown that the procedure proposed by Stoer and Bulirsch is very efficient for the problem to be solved here (cf. [4] and [5]). For all of the procedures implemented, the proper adjustments were made to meet the additional algebraic constraints as well as the equidistant output of results.

The system of model elements described here was implemented in a calculation program. The program was written in C++ and primarily object oriented techniques were used. The user can arrange and combine individual elements as required and thus generate arbitrary configurations. The description of various operating conditions under investigation is also based on this procedure, making it possible to work out several different operating conditions in one successive computation run.

4 Parameter Determination

In order to use the procedure described here in practical applications, suitable parameters for the submodels must be identified. The goal of a simplified model mentioned above not only entails reducing model complexity in terms of the effort required for calculation, but also reducing the number of parameters required for the model.

Input parameters can be divided into three groups:

1. The first group consists of "standard parameters" such as masses, mass moments of inertia, load torques for the accessory drives and geometrical dimensions. Normally, it poses no problem to obtain these values since they are also required for other tasks and are easy to determine.

2. The second group contains quantities that require a little more effort to determine or those that are required exclusively for this calculation.

- One of the most important of these "problem-specific" quantities that is often unavailable in a suitable form is the cyclic irregularity of the crankshaft. To perform simulation calculations, it must be available as a time series or a Fourier series for the operating points desired (i.e. constant engine speeds). These data are ideally obtained by measuring an engine prototype whose belt drive is to be analyzed. However prototype engines are often unavailable, and recourse must be taken to data obtained for a similar engine. In this case quantitative conclusions from simulation results are not as accurate. In practical applications, the degree of irregularity for various operating speeds is often indicated. This is insufficient since these represent only the real part of the complex Fourier coefficients that are required. If this data is used, it must also be assumed that a one-order excitation is present. A further inaccuracy is introduced by the assumption that the belt drive does not affect the cyclic irregularity of the crankshaft.
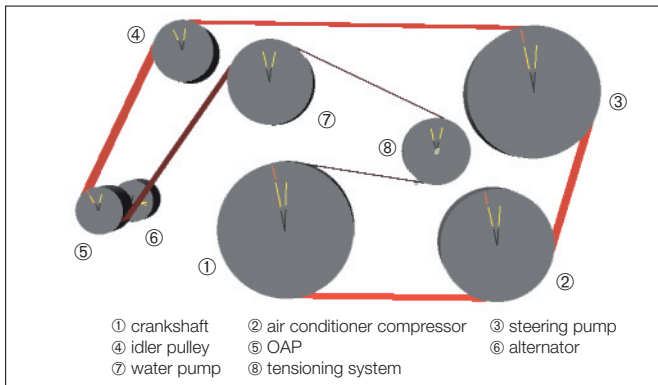
Figure 7   Belt drive example

① crankshaft   ② air conditioner compressor   ③ steering pump
④ idler pulley   ⑤ OAP   ⑥ alternator
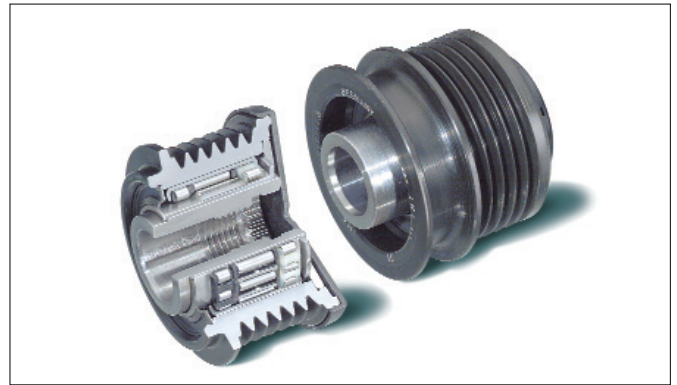⑦ water pump   ⑧ tensioning system

Figure 8   INA's overrunning alternator pulley

- The stiffness and damping parameters for hydraulic tensioning systems are also important model quantities that cannot be determined from design data directly. For this reason, these tensioner parameters are determined from tests in which mappings, i.e. force-displacement diagrams under defined conditions (amplitude and frequency of displacement excitation), are prepared (Figure 6a and 6b). The testing situation is then imitated using a standard set of data for the simulation program. The stiffness and damping values for the tensioner are adjusted until the same mapping is obtained for both simulation and test.

- Unlike hydraulic systems, the determination of parameters for mechanical tensioning systems is comparatively simple since they can be read off from the mapping directly.

- The OAP must be measured separately to achieve the nonlinear stiffness function. The effort required for this is determined by the high degree of accuracy required for the small twisting angles.

3. The third group of model parameters normally cannot be measured, e.g. belt damping parameters or the friction values for the contact between the belt and the pulley. The reason for this difficulty is that these parameters are not directly accessible from a measuring standpoint. Among other things, this results from the model itself. In reducing model complexity, a small number of parameters must be used to reflect processes that are much more complicated than can be depicted for the physical equivalent in the model. In the experiment, a generalization such as this or a "skewing" of physical effects cannot be understood in exactly the same way. In cases like these, the investigator must rely on adjustment calculations. Starting with an application that matches the target system as closely as possible and for which measurements are available, replacement parameters are adjusted for the entire system to reflect real-life conditions more closely. This process is similar to that described for the "hydraulic tensioner" subsystem.

5 Comparison of measurements and calculations

The application example used to illustrate the simulation program discussed here is the accessory drive that is mass produced for a 4-cylinder diesel engine (Figure 7). An air conditioner compressor, the alternator and the water pump are driven from the crankshaft by means of a single belt. The arrangement specified for the accessory drive is such that an idler pulley between the steering pump and the alternator is necessary.

A one-way clutch is integrated in the alternator pulley. It serves to increase belt life and to reduce belt drive vibrations and noise (Figure 8). The tension pulley is arranged on the slack side of the drive as usual, and the overrunning alternator pulley (OAP) allows a mechanical tensioning system to be used.

Measured values for the cyclic irregularity of the crankshaft were available for this engine for some engine speeds between 630 and 1700 min^{-1}. Adequate Fourier coefficients were determined from these data to specify the motion in the simulation.
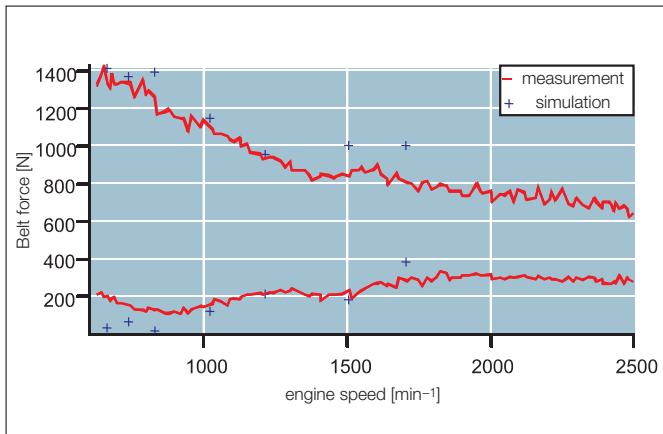
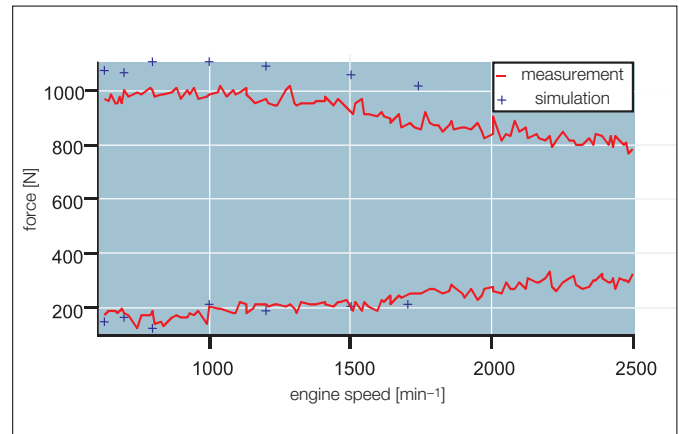Figure 9   Belt forces on the idler pulley

Figure 10   Forces on the tensioner

5.1 Belt forces

The level of belt forces is an important quantity in the design of accessory drives. Finding the right compromise is complicated by conflicting interests: On the one hand, the loads on the accessory drive bearing supports and on the belt should be reduced by lower belt forces. At the same time, however, sufficient reserves are required to transmit the necessary load and accelerating torque in order to avoid premature wear to the belt due to slip.

The maximum belt forces, particularly on the load side of the belt, greatly exceed the value of the static preload. Typically, preload is in the 200 to 350 N range. On the other hand, dynamic forces of up to 1,400 N occur on the operating drive idler pulley – both in the measurements and in the simulation (Figure 9).

5.2 Tension-pulley forces

An agreement similar to that found for the forces acting on the idler pulley can be observed for the minimum and maximum tension-pulley forces. The maximum forces in the simulation, however, are approx. 100 N higher than the measured values (Figure 10).

The amplitude of the tensioning lever is also represented correctly except for an increase of approx. 1 mm in the lower speed range (Figure 11).

5.3 Belt vibration

It is quite difficult to verify transversal vibrations for single belt spans due to the extremely narrow frequency ranges in which these phenomena occur. This is because the distance between break points in the engine speed range is normally so large that potential problem areas may not be recognized correctly. If measurements for the excitation (cyclic

irregularity of the crankshaft) vs. engine speed are not available, then the investigator must rely on the interpolation of Fourier coefficients. It has been observed that a sufficient distribution of the frequency content for the excitation will greatly simplify the recognition of belt span vibrations. In some cases, it is not possible to recognize vibrations until this distribution is made.

In the drive under investigation, belt span vibrations between the steering pump and the idler pulley were observed in the experiment at approximately 800 min⁻¹. These vibrations did not occur in the calculations for this speed. In order to allow the simulation of the system for different speeds in a range close to the given value, the 800 min⁻¹ Fourier coefficients were used for those speeds as well. In this way, belt vibrations in the simulation were observed that had the same magnitude as those in the test. The time series (Figure 12) shows highly fluctuating vibration frequencies that are caused by corresponding time-variant longitudinal forces in the belt span. This effect – also evidenced experimentally – is depicted correctly in the model formulation selected.

5.4 Slip

Besides the "natural" slip component, which is necessary for power transfer, no significant slippage was observed in the belt drive analyzed here. This was the case for both the measurement and the simulation. The reason for the difference between the (low) slip values for the measurement and the calculation is that a relative motion between belt and pulley does not occur in the model until the belt slides through the entire belt wrap range. In reality, slippage always occurs locally in the belt's input and output range. In a series of applications it was demonstrated that – compared to other applications – any potential slippage in the drive can be predicted (disregarding the low absolute slip values in the simulation that result from the model).

5.5 OAP

The good performance and effectiveness of the OAP of the drive under investigation are readily apparent when the angular velocities of the belt pulley and the alternator shaft are compared. This is true for both measurement and the simulation. In the phase in which the belt
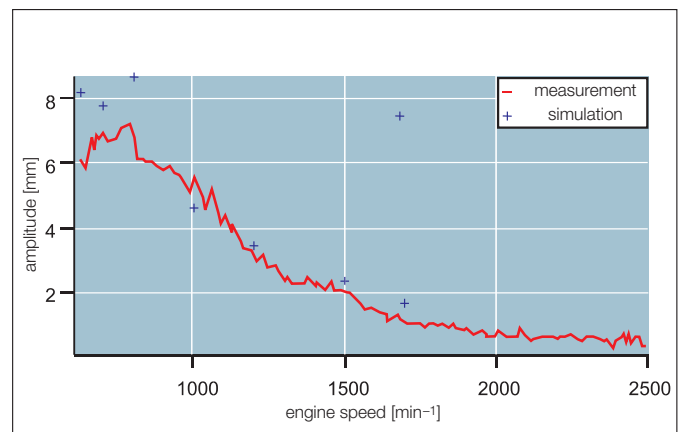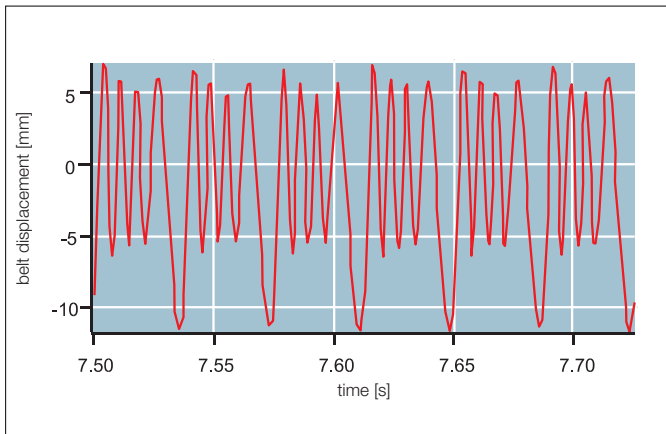

Figure 11   Amplitude of tensioner lever

Figure 12 Belt vibrations between steering pump and idler pulley (simulation)
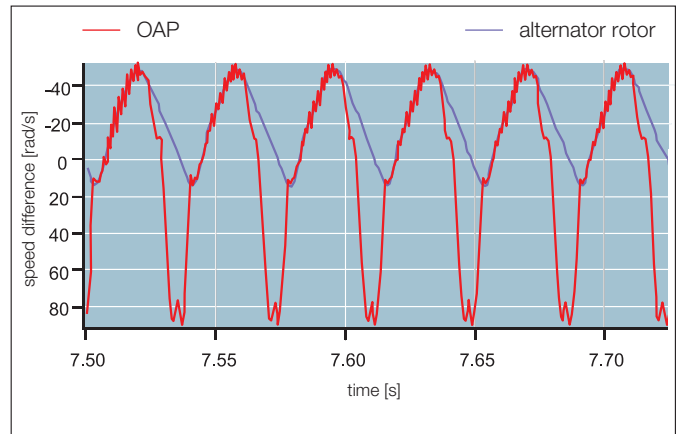

Figure 13 Behavior of the OAP (simulation)

pulley's speed decreases, the alternator is disengaged; its deceleration corresponds to the load and frictional torques and is usually much lower than that of the belt pulley.

When the belt pulley begins to accelerate, the alternator still has a comparatively higher speed. It is not until the belt pulley has attained the alternator speed that clutch engages again and rotates the alternator for the rest of the acceleration phase. (Figure 13).

The cyclic irregularity of the alternator is significantly reduced, while its mean speed increases by a small percentage.

Apparently, the effect described here abates as alternator load increases and the maximum deceleration decreases. In practical applications it is most significant for low to medium alternator loads and engine speeds up to approx. 1,500 min^{-1}.

6 Conclusion

Although the model presented in this paper depicts a quite simplified view of physical processes in places, impressive evidence of its validity can be seen in the comprehensive simulation of relevant processes at work in the accessory drive. It has thus been possible to find a highly practical compromise between effort (both in terms of development and applications engineering) and utilization, i.e. computational reliability.

Literature

[1] Fritzer, A.:
Entwicklung von Modellen und Berechnungsverfahren zur Bestimmung der Schwingungsbelastungen in Steuer- und Hilfsantrieben von Verbrennungsmotoren, Abschlußbericht des Forschungsvorhabens „Steuerungsantrieb", AIF-Nr. 7470, Forschungsvereinigung Verbrennungskraftmaschinen e.V., Frankfurt/Main 1991

[2] Herrmann, R.-J.:
Ermittlung und systematische anwenderorientierte Darstellung von dynamischen und quasistatischen Kennwerten von Keil-, Flach- und Zahnriemen-Getrieben, Abschlußbericht des Forschungsvorhabens „Riemenkennwerte", AIF-Nr. 7453, Forschungskuratorium Maschinenbau e.V., Frankfurt/Main 1991

[3] Funk, W.:
Zugmittelgetriebe. Springer Verlag. Berlin. 1995

[4] Press, W. H.; et al.:
Numerical Recipes. Cambridge University Press. Cambridge 1986

[5] Stoer, J.; Bulirsch, R.:
Numerische Mathematik 2nd, 3nd ed. Springer Verlag. Berlin. 1990

Authors

Peter Solfrank is Department Manager of Valve Train Components – Product Development/Calculation at INA Motorenelemente Schaeffler KG in Hirschaid, Germany.
His E-mail address is: solfrpte@ina.de

Peter Kelm is a Calculation Engineer in the Product Development/CAE Development Department at INA Wälzlager Schaeffler oHG in Herzogenaurach, Germany.
His E-mail address is: kelmpte@ina.de

INA Wälzlager Schaeffler oHG

91072 Herzogenaurach (Germany)
Telephone (+49 91 32) 82-0
Fax (+49 91 32) 82-49 50
http://www.ina.com